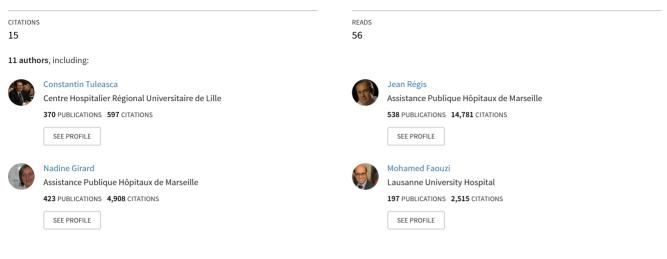
See discussions, stats, and author profiles for this publication at: https://www.researchgate.net/publication/322504840

# Clinical response to Vim's thalamic stereotactic radiosurgery for essential tremor is associated with distinctive functional connectivity patterns

Article in Acta Neurochirurgica · January 2018 DOI: 10.1007/s00701-017-3456-x



Some of the authors of this publication are also working on these related projects:

Exploring brain communication pathways by combining diffusion based quantitative structural connectivity and EEG source imaging View project

Brain Folding Patterns View project

```
All content following this page was uploaded by Constantin Tuleasca on 28 July 2019
```

# Clinical response to Vim's thalamic stereotactic radiosurgery for essential tremor is associated with distinctive functional connectivity patterns

Constantin Tuleasca<sup>1,2,3,8</sup>, MD, Elena Najdenovska<sup>\*2</sup>, MSc, Jean Régis<sup>4\*</sup>, MD, Tatiana

Witjas<sup>5</sup>, MD, Nadine Girard<sup>6</sup>, MD, PhD, Jérôme Champoudry<sup>4</sup>, MSc, Mohamed Faouzi<sup>7</sup>,

PhD, Jean-Philippe Thiran<sup>3,9,10</sup>, PhD, Meritxell Bach Cuadra<sup>2,3</sup>, PhD, Marc Levivier<sup>1,9</sup>, MD,

PhD, IFAANS, AND Dimitri Van De Ville<sup>8,11</sup>, PhD

<sup>1</sup>Centre Hospitalier Universitaire Vaudois (CHUV), Neurosurgery Service and Gamma Knife Center, Lausanne, Switzerland; <sup>2</sup>Medical Image Analysis Laboratory (MIAL) and Department of Radiology-Center of Biomedical Imaging (CIBM), Centre Hospitalier Universitaire Vaudois, Lausanne, Switzerland; <sup>3</sup>Signal Processing Laboratory (LTS 5), Ecole Polytechnique Fédérale de Lausanne (EPFL), Switzerland; <sup>4</sup>Stereotactic and Functional Neurosurgery Service and Gamma Knife Unit, CHU Timone, Marseille, France; <sup>5</sup>Neurology Department, CHU Timone, Marseille, France; <sup>6</sup>AMU, CRMBM UMR CNRS 7339, Faculté de Médecine et APHM, Hopital Timone, Department of Diagnostic and Interventionnal Neuroradiology, Marseille; <sup>7</sup>Institute of Social and Preventive Medicine, Lausanne, Switzerland; <sup>8</sup>University of Geneva, Faculty of Medicine, Switzerland; <sup>9</sup>University of Lausanne, Faculty of Biology and Medicine; <sup>11</sup>Centre Hospitalier Universitaire Vaudois, Department of Radiology; <sup>12</sup>Medical Image Processing Laboratory, Ecole Polytechnique Fédérale de Lausanne (EPFL), Switzerland; \*Equally contributors as second author:

# **Corresponding author:**

Constantin Tuleasca, MD, MD-PHD candidate, Centre Hospitalier Universitaire Vaudois, Neurosurgery Service and Gamma Knife Center, Rue du Bugnon 44-46, BH-08, CH-1011, Lausanne, Switzerland; Tel: +41-21-314-26-02; Fax: +41-21-314-11-99; e-mail: constantin.tuleasca@gmail.com; dimitri.vandeville@epfl.ch

# Abstract

**Introduction:** Essential tremor (ET) is the most common movement disorder. Drug-resistant ET can benefit from standard procedures (deep brain stimulation, thalamotomy) or minimally invasive high-intensity focused ultrasound (HIFU) or stereotactic radiosurgical thalamotomy (SRS-T). Resting state fMRI (rs-fMRI) is a non-invasive imaging method acquired in absence of a task. We examined whether rs-fMRI correlates with tremor score on the treated hand (TSTH) improvement 1 year after SRS-T.

**Methods:** We included 17 consecutive patients treated with left unilateral SRS-T in Marseille, France. Tremor score evaluation and rs-fMRI were acquired at baseline and 1 year after SRS-T. Resting-state data (34 scans) were analyzed without *a priori* hypothesis, in Lausanne, Switzerland. Based on degree of improvement in TSTH, to consider SRS-T at least as effective as medication, we separated two groups: 1, <= 50% (n=6, 35.3%); 2, > 50% (n=11, 64.7%). They did not differ statistically by age (p=0.86), duration of symptoms (p=0.41) or lesion volume at 1 year (p=0.06).

**Results:** We report TSTH improvement correlated with interconnectivity strength between salience network with left claustrum and putamen, as well as between bilateral motor cortices with right visual association area (the former also with lesion volume). Longitudinal changes showed additional associations in inter-connectivity strength between right dorsal attention network with ventro-lateral prefrontal cortex and salience network with fusiform gyrus.

**Conclusions:** Brain connectivity measured by resting-state fMRI relates to clinical response after SRS-T. Relevant networks are visual, motor and attention. Inter-connectivity between visual and motor areas is a novel finding, revealing implication in movement sensory guidance.

**Key words:** resting-state, fMRI, essential tremor, ventro-intermediate nucleus, radiosurgery, independent component analysis, thalamotomy

# INTRODUCTION

Essential tremor (ET) is the most common movement disorder. Cardinal feature is tremor, occurring during voluntary movements of the upper extremities, additionally affecting the trunk, head and voice[30]. It has been hypothesized that abnormal oscillations appearing within so-called "tremor network", involving ipsilateral motor area, ventro-intermediate nucleus (Vim) and red nucleus, and contralateral cerebellum (e.g., dentate nucleus) are driving tremor, but exact cause is still a matter of debate[31, 32].

The first line treatment is pharmacological. If resistance/side-effects to medication occur, neurosurgical intervention is considered. The target is the Vim[4, 9, 13]. *Gold standard* open surgical interventions are deep brain stimulation (DBS) and radiofrequency thalamotomy both immediately effective at suppressing tremor[4, 22]. Minimally invasive alternatives are high-intensity focused ultrasound (HIFU) and stereotactic radiosurgical thalamotomy (SRS-T)[29, 44]. Radiosurgery (RS), unlike open surgery, induces progressive tremor arrest (maximum delay up to 1 year latter)[13, 26, 43].

Functional MRI (fMRI) is a powerful imaging technique, which can be used to study task-based or spontaneous activity. In particular, spontaneous fluctuations are informative about functional network organization, such as the motor network, as shown by early seminal work of Biswal et al.[8]. This field has great potential for clinical studies, due to minimal necessity for patient compliance and powerful new analytic tools, that can extract rich information from resting state fMRI (rs-fMRI)[19], thus opens avenues towards imaging-based biomarkers in multiple pathologies, including ET[5, 10, 17, 20]. Functional connectivity (FC) or inter-connectivity (IC) has been classically defined as the temporal correlations between spatially remote neurophysiological events, as a deviation from statistical independence across these events, in distributed neuronal groups and areas[19].

In the present study, we used rs-fMRI to non-invasively investigate the effect of SRS-T on brain networks, by using a methodology implying no *a priori* hypothesis, and a standard type of analysis. We carried out independent component analysis (ICA) to extract relevant networks and examine longitudinal changes in these networks that are correlated with treatment response. We expected that resting-state fMRI longitudinal changes relate to tremor arrest after SRS-T.

# METHODS

# Patients

We prospectively included 17 consecutive patients (right-sided tremor, drug-resistant, fulfilling table 1 criteria) treated only with left unilateral SRS-T in Marseille, France, between September 2014 and August 2015. This study received approval (CHU Timone, CPPRB1) from the Ethical Committee of the Marseille University Hospital. Written informed consent was obtained from all patients (inclusion criteria, table 1). All cases were referred by a movement disorders neurologist (TW).

Baseline tremor (by TW) and neuroimaging assessment (on a single 3 T MR machine, Siemens Skyra, Munich, Germany, T1 and rs-fMRI, n=17) was performed. The vast majority of patients didn't have medication anymore, usually for inefficacy reasons. However, the clinical evaluation was done under the pharmacological therapy (if one had such in a minority of situations), while the scanning in the drug-naïve state. Same protocol was repeated one year after SRS-T (n=17). The mean age was 70.1 years (range 49-82). The mean duration of symptoms was 38 years (range 6-70) (table 2). The mean time to tremor improvement in the present series was 3.32 months [standard deviation (std) 2.7, range 0.2-10].

# Clinical evaluation and outcome measures

Clinical evaluation was made using validated and well-established outcome measures, every three months after SRS-T. Tremor severity was assessed using questionnaire designed by Bain *et al.*[2] (e.g. activities of daily living (ADL))[2], tremor score on right treated hand (TSTH, e.g., right), from Fahn-Tolosa-Marin tremor rating scale[15] and head tremor score (table 2 for demographic data).

# Stereotactic radiosurgical thalamotomy procedure

All SRS-T procedures were performed by same neurosurgeon (JR), using the Leksell Gamma Plan software. Non-stereotactic images, including diffusion tensor diffusion data, acquired before the treatment, were co-registered with the stereotactic ones. After application of Leksell® coordinate G Frame (Elekta AB, Stockholm, Sweden), all patients underwent stereotactic CT and MRI. Anterior and posterior commissure (AC and PC) were defined on the magnetic resonance ventriculography (T2 Ciss/Fiesta sequence). Indirect targeting was performed using standard methodology by Guiot's diagram, placed 2.5 mm above the AC-PC line and 11 mm lateral to the wall of third ventricle. A single 4-mm isocenter was used and a

maximal prescription dose of 130 Gy, as well as beam blocking to optimize the gradient of dose toward the internal capsule[27, 40-42, 44].

# **MRI** data acquisition

Imaging was done on head-only 3T magnetic resonance imaging (MRI) scanner, SIEMENS SKYRA (Munich, Germany, 32-channel receive-only phased-array head coil): native (before SRS-T) and Gadolinium contrast-enhanced T1-weighted (T1w, after SRS-T) and resting-state fMRI images. The following parameters were employed: T1w-TR/TE=2300/2·98ms, isotropic voxel of 1mm<sup>3</sup>, 160 slices; T2\*-weighted fast echo planar imaging (BOLD contrast, before the Gadolinium injection)- TR/TE =  $3\cdot3s/30$  ms/90 degrees), voxel size 4 x 4 x 4 mm<sup>3</sup>, 300 volumes acquired per subject), 46 interleaved axial slices. The rs-fMRI experiments, acquired with no explicit task, consisted of a 10-min run, in which participant were asked to relax with their eyes closed, without falling asleep or engaging in cognitive or motor tasks. In addition, a field map was acquired to correct for the effect of field inhomogeneity.

# Resting-state fMRI data preprocessing and motion scrubbing

Processing of fMRI data was performed using different standard software suites: Statistical parametric Mapping (SPM12, <u>http://www.fil.ion.ucl.ac.uk/spm/</u>, Welcome Trust Center for Neuroimaging, London, UK). Functional scans were realigned to the first scan of the series. Since motion is an important potential confounding factor in these clinical populations, we computed Power's framewise displacement index for each time point[34]. When it exceeded 0.5mm, the corresponding frame was "scrubbed" along with one proceeding and two following ones (for a total of 5 for one time-point exceeding the upper limit allowed). Only the remaining frames were further considered. At baseline, the mean number of frames taken out was 35 (median 15, range 0-135) and at 1 year was also 35 (median 15, range 0-150). Then, the images were spatially normalized into the standard anatomical space as defined by the Montreal Neurological Institute (SPM-MNI, Canada) and spatially smoothed using a Gaussian filter with a full width at high maximum (FWHM) of 6 mm. The voxel size generated from the above acquisition parameters was oversampled to 2 x  $2 \times 2 \text{ mm}^3$ .

No sedation was used, so as not to influence resting-state brain activity in any way.

#### Resting-state fMRI network extraction

Resting-state data was analyzed in Lausanne, Switzerland, by two persons not involved in patient selection, radiosurgery procedure or follow-up course (CT and DVD).

Group-level independent component analysis (ICA) was applied to decompose rsfMRI data into components of temporally coherent spontaneous activity using GIFT ICA Toolbox (USA, <u>http://icatb.sourceforge.net</u>)[11]. Data-driven analytic approach we employed considered the concatenated data of the 34 scans (17 subjects X 2, baseline and 1 year). Total number of components (c) was set to 20 (table 3), which is a setting commonly used in literature for identifying large-scale distributed networks (main figure 1). After visual inspection of maps at group level, 2 (components 1 and 3) out of 20 components were excluded. The other 18 were kept for subsequent analysis, as they showed neurologically relevant spatial patterns type (main figure 1, table 3).

# *Resting-state fMRI statistical analysis*

For rs-fMRI data, analysis of variance (ANOVA) was implemented in SPM12 (http://www.fil.ion.ucl.ac.uk/spm/software/spm12, London, United Kingdom) as a *flexible factorial model*, on each component, by using individual subject-level maps, to take into account time point (baseline *versus* 1 year after SRS-T), response (groups 1 and 2), and interactions between. Bonferoni correction was used to deal with number of models (20). We then report corrected *p*-values using conventional cluster-level family wise error (FWE) correction.

For correlation between IC values and previously detailed tremor scores, STATA version 11 (STATA Corp LLC, College Stations, TX, USA) was used.

# RESULTS

#### Group definition for further statistical analysis

Currently available medications improve tremor in approximately 50% of patients and Propranolol, most commonly used, reduces tremor amplitude by approximately 50%[33]. To consider a therapeutical effect of SRS-T at least as effective as medication, we conventionally divided patients in two groups: 1, <= 50% improvement in TSTH (n=6, 35.3%) and 2, > 50% improvement (n=11, 64.7%). There was no difference in age (p=0.86) or duration of symptoms (p=0.41) between groups. There was a tendency towards higher thalamotomy

volumes in group 2 (p=0.06, mean in group 1= 0.044 ml (std 0.04, range 0.002-0.127 ml); mean in group 2= 0.17 ml (std 0.187, range 0.027 - 0.600 ml).

# **Clinical result**

Overall ADL improvement was 82.9% (std dev 27.3, range 0-100%) and TSTH improvement was 67.3% (std dev 28.2, range 13.3-100%).

# Radiological outcome: lesion volume after thalamotomy

The thalamotomy volume has been drawn on the T1 (Gadolinium-injected) MR, 1 year after SRS-T, which is considered the definitive radiological answer in our experience[43]. To ensure the accuracy of this volume calculation, each patient MR at 1-year follow-up was imported in the Leksell GammaPlan software (Elekta instruments, AB, Sweden) and co-registered with the therapeutic images. We projected on the MR-signature the 90 Gy isodose line, which corresponds to the final radiological response, in our previously published experience[35, 43]. Manually, using the segmentation tools, the draw was made for the individual cases. The "volume" module inside the station was used to extract the values.

Mean lesion volume after SRS-T was 0.125 ml (standard deviation 0.162, range 0.002-0.600 ml). There was no correlation between ADL drop and lesion volume (p=0.17), but the former related with TSTH improvement (p=0.04).

# Cognitive assessment

Mean pretherapeutic Matthis Dementia Rating Scale[38] was 135.9 and posttherapeutic was 135.5 (p>0.05).

# Interaction between time-point (baseline versus 1 year) and clinical response Relevant regions: IC strength between default-mode network and bilateral insula (c9) with left claustrum and putamen<sup>1</sup>; bilateral motor cortex (c13) with right visual association cortex<sup>2</sup>

We report statistically significant IC within 2 networks. The first is salience, involving bilateral superior frontal gyri and insular areas (c9) with left claustrum and putamen (main figure 2, 2.1. - 2.4; main figure 3 for brief anatomical relevance). The second is bilateral motor network (c13) with right visual association cortex, right Brodmann area (BA) 19 (table 4; main figure 4, 4.1-4.6; main figure 5 for brief neuroanatomical relevance).

For left claustrum and putamen, corresponding boxplots and their median IC values are shown in main figure 2 (for IC values refer to table 5). At baseline, IC were positive in group 1 and remained further so, while being close to zero in group 2 (main figure 2, 2.1). Functional connectivity differences (between 1 year and baseline) actually related to TSTH improvement, allowing a separation of group 1 from group 2 (main figure 2, 2.2). An increase in IC at 1 year was associated with a better outcome (figure 2, 2.2). Furthermore, baseline IC correlated with the TSTH improvement percentage, from a range of 1.91 (13.3% improvement) to -0.46 (100% improvement) (Spearman's rank correlation coefficient=0.01, main figure 2, 2.3). Shorter disease duration was associated with better TSTH improvement and a IC value increase at 1 year, towards 1 (main figure 2, 2.4) (Spearman's rank correlation coefficient=0.02).

For right visual association area, corresponding boxplots and their median values are shown in figure 4. The IC values can be seen in detail in table 5. At baseline, they were negative in group 1 and inversely positive at 1 year, while being close to zero in group 2 (main figure 4, 4.1). A decrease in IC at 1 year was related to TSTH improvement, allowing a separation of group 1 from group 2 (main figure 4, 4.2). The baseline IC values predicted percentage of TSTH improvement, with positive values associated with a better outcome (range from -1.068 (13.3% improvement) to 1.065 (100% improvement)) (Spearman's rank correlation coefficient=0.01, main figure 4, 4.3). Furthermore, baseline head tremor score (figure 4, 4.4) correlated with baseline IC values (negative IC associated for both with higher tremor scores for both, Spearman's rank correlation coefficient=0.02). Interestingly, higher lesion volumes were associated both with higher difference in IC values between 1 year and baseline (figure 4, 4.5, Spearman's rank correlation coefficient=0.001) and also with higher baseline IC values (figure 4, 4.6, Spearman's rank correlation coefficient=0.01).

# Main effect of time point (baseline versus one year after SRS-T)

Relevant anatomical regions: IC strength between right dorsal attention network (c2) with left anterior ventro-lateral prefrontal cortex<sup>1</sup>; salience network (c9) with right fusiform gyrus (including V5)<sup>2</sup>

We report statistically significant IC within two networks. The first is right dorsal attention network (c2) with the left anterior ventro-lateral prefrontal cortex (VLPFC, main figure 6, 6.1 till 6.3; main figure 7 for brief anatomical relevance). The second is salience network (c9) IC with fusiform gyrus (main figure 8, 8.1. and 8.2) with a cluster including parts of right visual area V5 (main figure 9 for brief anatomical relevance, table 3 and 4).

For the VLPFC (main figure 6, 6.1 and 6.2 for their respective values), no or slight change in IC at 1 year after SRS-T correlated with better TSTH improvement (Spearman's rank correlation coefficient=0.01, main figure 6, 6.3).

For the right fusiform gyrus and visual area V5 (main figure 8, 8.1 and 8.2), the mean baseline IC values in group 1 were 0.33 (-1 to 1.10) and at 1 year passed to -0.30 (-0.69 to 0.28); for group 2 the mean was 0.02 (-0.86 to 0.93) and at 1 year passed to 0.27 (-1.07 to 2.46) (main figure 8, 8.1 and 8.2).

# Main effect of group (group 1 versus 2, independent of time-point)

Multiple differences were found between group 1 and group 2, independent of timepoint, involving the following relevant anatomical regions: cerebellum (comprising dentate nucleus), basal ganglia including thalamus (both right and left) and putamen, frontal lobe (encompassing frontal eye fields, dorso-lateral prefrontal cortex), parietal lobe (angular and supramarginal gyrus), temporal lobe (middle temporal area), occipital lobe (visual association areas, retrosplenial cortex), cingulate (both anterior dorsal and posterior). They are displayed in supplementary figures 1, 2, 3 (main figure 10 for neuro-anatomical relevance) and table 6. The corresponding boxplots present median values as well as the range for each group, at baseline and 1 year after SRS-T.

# Influence of confounders

For relevant IC values, there was no influence of age (p>0.05). The influence of disease duration was statistically significant only for c9 (see below). The thalamotomy volume correlated only with IC strength between bilateral motor areas (c13) with right visual association area (see below).

# DISCUSSION

To the best of our knowledge, this is the first study that uses rs-fMRI as a non-invasive neuro-imaging tool for evaluating clinical response after SRS-T. We considered both baseline and 1 year after SRS-T follow-up functional imaging, to be able to detect network changes related to therapeutic answer after SRS-T. We focused on improvement in TSTH, as SRS-T was performed only unilaterally in this cohort (left SRS-T for right hand).

We report TSTH improvement correlated with IC strength between salience network with left claustrum and putamen, as well as between bilateral motor cortex with right visual association area (former also with lesion volume). Longitudinal changes showed additional associations in IC strength between right dorsal attention network with ventro-lateral prefrontal cortex and salience network with fusiform gyrus. Relevant networks are visual, motor and attention. Inter-connectivity between visual and motor areas is novel finding, revealing implication in movement sensory guidance.

We briefly analyzed the neuroanatomical perspective of these relevant brain areas. The input and output of claustrum is related to almost all regions of cortex (including cingulate, visual areas in occipital lobe, enthorhinal cortex, and temporal areas)[14]. Furthermore, we identified that the anterior dorsal part, found here, connects with motor and somato-sensory cortex. Main functions include: cross-modal perception[12], coordination of matching between visual and tactile modalities[3], and has even been invoked as important to consciousness[14]. The putamen, by its connections to substantia nigra and globus pallidus, plays a major role in movement regulation, motor learning, preparation, sequences, tasks and amplitude, limb movement control, and as part of motor system that is mobilized to take action, or influences various types of learning[1]. Right visual association cortex (including V3, V4, V5) was interconnected with c13, bilateral motor network component. It has been previously hypothesized that visual areas must be linked to motor areas for sensory guidance of movement of hand and fingers[21], and further so in motor control. Several hypothesis warrant for further discussion. One possibility would be that corpus callosum actually mediates tasks in which the visual cortex on one part of the body is linked to contralateral motor cortex, in line with our findings. Another hypothesis would be visual input to caudate nucleus and claustrum[37], explaining appearance of the former in another component (see previous). Furthermore, a third possibility could be that cerebellum might play the essential role of calibrating the relationship between visual and somatosensory/motor information. Other functions of the visual association cortex are related to feature extraction, attentional and multimodal integrating functions. Furthermore, electrophysiology data suggest sensitivity to motion-delineated forms[39] and its role as a differentiation point between the 'what' and 'where' visual pathways. Additional involvement of the visual association cortex is in horizontal saccadic eye movements, visuospatial information processing, orientation-selective attention and tracking visual motion patterns[45].

The left VLPFC is considered the end-point of ventral pathway, which brings information about stimuli characteristics. In the present study, it is inter-connected with the right dorsal attention network. Recent studies have suggested a role in hand movements[36]. The fusiform gyrus, interconnected here with salience network, is mainly involved in high-

level vision as part of the ventral visual stream ("what" pathway) and various neural pathways related to recognition. It encompasses the middle temporal area (V5), and plays a major role in motion perception, integration of local motor signals into global percepts, and guidance of some eye movements. Major projections include eye movement-related areas (e.g. frontal eye fields). It is worth noting that both V5 and V6 have high myelin content, a characteristic that is usually present in brain structures involved in fast information transmission.

Essential tremor is currently considered a spectrum of clinical features, including both motor and non-motor elements[31]. These features are nicely represented by found group differences, involving multiple anatomical regions (main figure 6).

Only one previous study, not related to radiosurgery[24], evaluated the effect of Vim HIFU in 10 patients with drug-resistant ET, on brain networks. A major difference is that Vim HIFU produces an apparent lesion and clinical effect immediately, unlike SRS-T (which can develop up to one year after the procedure). This delayed effect could account for brain networks reorganization and plasticity. The authors of the HIFU study used graph analysis on rs-fMRI data and found whole brain effects/changes at a latter time point of 3 months after the intervention, on the right lateral inferior occipital cortex. Part of this cluster also appeared in the present study. Resting-state observational studies in ET, which are non-interventional, are not the primary focus of the present report[5, 10, 16-18, 28].

We used a data-driven method (i.e., ICA) that allows identifying resting-state networks without any *a priori* hypothesis. We did this so as to not evaluate a specific tremor network, nor probe the cerebello-thalamo-cortical pathway, which was beyond our purpose. While one would expect that Vim "suppression" by SRS-T has an impact only on the known motor network(s), we presently report changes within remote areas, including purely motor, visuomotor areas, and areas related to cognition. These network changes 1 year after SRS-T are related to tremor improvement. In this sense, they might play a major, underestimated, physiopathological role, either because of a particular baseline phenotype[31], or by adaptive changes to intervention itself.

We reported an interesting connection between visual association areas and motor cortex in our ET patients, in the clinical context of impairment of sensory guidance of movement, including of hand and fingers. In fact, additional visual attention deficits or dysfunction in hand-eye coordination and ocular movements are considered as non-motor features in ET[6]. It is known that visual attention is of high importance for visual perception and for all the things we put perception to, including learning, memory and our interactions with the visual world[7]. It is worth noting that top-down signals come from multiple frontal

and parietal regions, but their "competition" is ultimately resolved within the visual cortex[25].

Our study has several potential limitations. One is the small number of subjects. Another, related to study design, is the use of resting-state data, which might not be directly related to motor performance; however, we aimed at studying network changes in the absence of a task. A third one is the lack of data on longitudinal changes (at baseline and 1 year) in a healthy control group; nevertheless, recent studies have advocated the reproducibility of functional networks across multiple sessions, including 1 year apart[23]. Furthermore, neurological evaluation was not blinded. Also, at which exact time point SRS-T induces these changes in brain networks remains unknown. The anatomical location of some clusters, such as the claustrum, should be carefully interpreted, due to the relatively low resolution of the fMRI in general.

# CONCLUSION

In conclusion, we report that a focal Vim lesion, produced by SRS-T, is correlated with a distinct functional connectivity pattern, implying changes not only within parts of the pure widely known motor loop, but also on remote areas, including primarily motor (claustrum, putamen; interconnected with salience network) and visual (occipital association cortex; interconnected with bilateral motor cortex) area. Using longitudinal data, at baseline and one year after SRS-T, we suggest that rs-fMRI relates to clinical response. The main areas involved include motor and visual networks, but also cognitive regions, mainly involved in attention (e.g., salience, dorsal attention), suggesting the connection between the former in sensory guidance of movements of hands and fingers.

<u>Funding:</u> The work was supported by the Swiss National Science Foundation (SNSF-205321-157040) and by the Centre d'Imagerie BioMédicale (CIBM) of the University of Lausanne (UNIL), the Swiss Federal Institute of Technology Lausanne (EPFL), the University of Geneva (UniGe), the Centre Hospitalier Universitaire Vaudois (CHUV), the CHU Timone, Marseille, France; the Hôpitaux Universitaires de Genève (HUG), and the Leenaards and Jeantet Foundations.

Acknowledgments: We acknowledge the contribution of Axelle Cretol, from Marseille University Hospital (CHU Timone), France who, as research assistant, kept the database up-

to-date

**Conflict of interest:** All authors certify that they have no affiliations, with or involvement in any organization or entity with any financial interest (such as honoraria; educational grants; participation in speakers' bureaus; membership, employment, consultancies, stock ownership, or other equity interest; and expert testimony or patent-licensing arrangements), or non-financial interest (such as personal or professional relationships, affiliations, knowledge or beliefs) in the subject matter or materials discussed in this manuscript.

**Ethics approval:** Ethical Committee of the Marseille University Hospital (CPPRB1) approved our study.

# References

 Alexander GE, Crutcher MD (1990) Functional architecture of basal ganglia circuits: neural substrates of parallel processing. Trends in neurosciences 13:266-271
Bain PG, Findley LJ, Atchison P, Behari M, Vidailhet M, Gresty M, Rothwell JC,

Thompson PD, Marsden CD (1993) Assessing tremor severity. Journal of neurology, neurosurgery, and psychiatry 56:868-873

3. Banati RB, Goerres GW, Tjoa C, Aggleton JP, Grasby P (2000) The functional anatomy of visual-tactile integration in man: a study using positron emission tomography. Neuropsychologia 38:115-124

4. Benabid AL, Pollak P, Gao D, Hoffmann D, Limousin P, Gay E, Payen I, Benazzouz A (1996) Chronic electrical stimulation of the ventralis intermedius nucleus of the thalamus as a treatment of movement disorders. Journal of neurosurgery 84:203-214

5. Benito-Leon J, Louis ED, Romero JP, Hernandez-Tamames JA, Manzanedo E, Alvarez-Linera J, Bermejo-Pareja F, Posada I, Rocon E (2015) Altered Functional Connectivity in Essential Tremor: A Resting-State fMRI Study. Medicine 94:e1936

6. Bermejo-Pareja F, Puertas-Martin V (2012) Cognitive features of essential tremor: a review of the clinical aspects and possible mechanistic underpinnings. Tremor and other hyperkinetic movements 2

7. Bisley JW (2011) The neural basis of visual attention. The Journal of physiology 589:49-57

8. Biswal B, Yetkin FZ, Haughton VM, Hyde JS (1995) Functional connectivity in the motor cortex of resting human brain using echo-planar MRI. Magnetic resonance in medicine 34:537-541

9. Blomstedt P, Hariz GM, Hariz MI, Koskinen LO (2007) Thalamic deep brain stimulation in the treatment of essential tremor: a long-term follow-up. British journal of neurosurgery 21:504-509

10. Buijink AW, van der Stouwe AM, Broersma M, Sharifi S, Groot PF, Speelman JD, Maurits NM, van Rootselaar AF (2015) Motor network disruption in essential tremor: a

functional and effective connectivity study. Brain : a journal of neurology 138:2934-2947

11. Calhoun VD, Adali T, Pearlson GD, Pekar JJ (2001) A method for making group inferences from functional MRI data using independent component analysis. Human brain mapping 14:140-151

12. Calvert GA (2001) Crossmodal processing in the human brain: insights from functional neuroimaging studies. Cerebral cortex 11:1110-1123

13. Campbell AM, Glover J, Chiang VL, Gerrard J, Yu JB (2015) Gamma knife stereotactic radiosurgical thalamotomy for intractable tremor: a systematic review of the literature. Radiotherapy and oncology : journal of the European Society for Therapeutic Radiology and Oncology 114:296-301

Crick FC, Koch C (2005) What is the function of the claustrum? Philosophical transactions of the Royal Society of London. Series B, Biological sciences 360:1271-1279
Fahn S, Tolosa E, Marin C (1988) Clinical rating scale for tremor. Parkinson's

Disease and Movement Disorders. Baltimore: Urban and Schwarzenberg, pp 225–234 16. Fang W, Chen H, Wang H, Zhang H, Liu M, Puneet M, Lv F, Cheng O, Wang X, Lu X, Luo T (2015) Multiple Resting-State Networks Are Associated With Tremors and Cognitive Features in Essential Tremor. Movement disorders : official journal of the Movement Disorder Society 30:1926-1936

17. Fang W, Chen H, Wang H, Zhang H, Puneet M, Liu M, Lv F, Luo T, Cheng O, Wang X, Lu X (2016) Essential tremor is associated with disruption of functional connectivity in the ventral intermediate Nucleus--Motor Cortex--Cerebellum circuit. Human brain mapping 37:165-178

18. Fang W, Lv F, Luo T, Cheng O, Liao W, Sheng K, Wang X, Wu F, Hu Y, Luo J, Yang QX, Zhang H (2013) Abnormal regional homogeneity in patients with essential tremor revealed by resting-state functional MRI. PloS one 8:e69199

19. Fox MD, Raichle ME (2007) Spontaneous fluctuations in brain activity observed with functional magnetic resonance imaging. Nature reviews. Neuroscience 8:700-711

20. Gallea C, Popa T, Garcia-Lorenzo D, Valabregue R, Legrand AP, Marais L, Degos B, Hubsch C, Fernandez-Vidal S, Bardinet E, Roze E, Lehericy S, Vidailhet M, Meunier S (2015) Intrinsic signature of essential tremor in the cerebello-frontal network. Brain : a journal of neurology 138:2920-2933

21. Glickstein M (2000) How are visual areas of the brain connected to motor areas for the sensory guidance of movement? Trends in neurosciences 23:613-617

22. Goldman MS, Ahlskog JE, Kelly PJ (1992) The symptomatic and functional outcome of stereotactic thalamotomy for medically intractable essential tremor. Journal of neurosurgery 76:924-928

23. Guo CC, Kurth F, Zhou J, Mayer EA, Eickhoff SB, Kramer JH, Seeley WW (2012) One-year test-retest reliability of intrinsic connectivity network fMRI in older adults. NeuroImage 61:1471-1483

24. Jang C, Park HJ, Chang WS, Pae C, Chang JW (2016) Immediate and Longitudinal Alterations of Functional Networks after Thalamotomy in Essential Tremor. Frontiers in neurology 7:184

25. Kastner S, Ungerleider LG (2000) Mechanisms of visual attention in the human cortex. Annual review of neuroscience 23:315-341

26. Kondziolka D, Ong JG, Lee JY, Moore RY, Flickinger JC, Lunsford LD (2008) Gamma Knife thalamotomy for essential tremor. Journal of neurosurgery 108:111-117

27. Lefranc M, Carron R, Regis J (2015) Prelemniscal Radiations: A New Reliable Landmark of the Thalamic Nucleus Ventralis Intermedius Location. Stereotactic and functional neurosurgery 93:400-406

28. Lenka A, Bhalsing KS, Panda R, Jhunjhunwala K, Naduthota RM, Saini J, Bharath RD, Yadav R, Pal PK (2017) Role of altered cerebello-thalamo-cortical network in the neurobiology of essential tremor. Neuroradiology 59:157-168

29. Lipsman N, Schwartz ML, Huang Y, Lee L, Sankar T, Chapman M, Hynynen K, Lozano AM (2013) MR-guided focused ultrasound thalamotomy for essential tremor: a proof-of-concept study. The Lancet. Neurology 12:462-468

30. Louis ED (2005) Essential tremor. The Lancet. Neurology 4:100-110

31. Louis ED (2009) Essential tremors: a family of neurodegenerative disorders? Archives of neurology 66:1202-1208

32. Louis ED (2016) Essential Tremor with Head Tremor: Trait or State? The Canadian journal of neurological sciences. Le journal canadien des sciences neurologiques 43:443-444

33. Lyons KE, Pahwa R (2008) Pharmacotherapy of essential tremor : an overview of existing and upcoming agents. CNS drugs 22:1037-1045

34. Power JD, Barnes KA, Snyder AZ, Schlaggar BL, Petersen SE (2012) Spurious but systematic correlations in functional connectivity MRI networks arise from subject motion. NeuroImage 59:2142-2154

35. Regis J, Carron R, Park M (2010) Is radiosurgery a neuromodulation therapy? : A 2009 Fabrikant award lecture. Journal of neuro-oncology 98:155-162

36. Rizzolatti G, Fogassi L, Gallese V (2002) Motor and cognitive functions of the ventral premotor cortex. Current opinion in neurobiology 12:149-154

37. Saint-Cyr JA, Ungerleider LG, Desimone R (1990) Organization of visual cortical inputs to the striatum and subsequent outputs to the pallido-nigral complex in the monkey. The Journal of comparative neurology 298:129-156

38. Schmidt R, Freidl W, Fazekas F, Reinhart B, Grieshofer P, Koch M, Eber B, Schumacher M, Polmin K, Lechner H (1994) The Mattis Dementia Rating Scale: normative data from 1,001 healthy volunteers. Neurology 44:964-966

39. Tardif E, Richer L, Bergeron A, Lepore F, Guillemot JP (1997) Spatial resolution and contrast sensitivity of single neurons in area 19 of split-chiasm cats: a comparison with primary visual cortex. The European journal of neuroscience 9:1929-1939

40. Tuleasca C, Pralong E, Najdenovska E, Cuadra MB, Marques JRF, Vingerhoets F, Regis J, Bloch J, Levivier M (2017) Deep brain stimulation after previous gamma knife thalamotomy of the Vim for essential tremor is feasible! Clinical, electrophysiological and radiological findings. Acta neurochirurgica 159:1371-1373

41. Tuleasca C, Witjas T, Najdenovska E, Verger A, Girard N, Champoudry J, Thiran JP, Van de Ville D, Cuadra MB, Levivier M, Guedj E, Regis J (2017) Assessing the clinical outcome of Vim radiosurgery with voxel-based morphometry: visual areas are linked with tremor arrest! Acta neurochirurgica 159:2139-2144

42. Tuleasca C, Witjas T, Van de Ville D, Najdenovska E, Verger A, Girard N, Champoudry J, Thiran JP, Cuadra MB, Levivier M, Guedj E, Regis J (2017) Right Brodmann area 18 predicts tremor arrest after Vim radiosurgery: a voxel-based morphometry study. Acta neurochirurgica

43. Witjas T, Carron R, Azulay JP, Regis J (2013) Gammaknife Thamamotomy For Intractable Tremors: Clinical Outcome And Correlations With Neuroimaging Features. MDS 17th International Congress of Parkinson's Disease and Movement Disorders, vol Volume 28, p 1247 44. Witjas T, Carron R, Krack P, Eusebio A, Vaugoyeau M, Hariz M, Azulay JP, Regis J (2015) A prospective single-blind study of Gamma Knife thalamotomy for tremor. Neurology 85:1562-1568

45. Zeki S (1993) The visual association cortex. Current opinion in neurobiology 3:155-159

**Main figure 1:** A total number of 20 components (c) with their respective networks were separated using visual evaluation both of their spatial profile and time-course: c2, right dorsal attention, in mirror with c16, left dorsal attention; c4, temporal pole, insula and retro-splenial cortex; c5, cerebellar; c6, bilateral occipital and parietal; c7, brainstem; c8, brainstem and cerebellar; c9, the frontal anterior part of the default mode network (DMN); c10, cerebellar and thalamic; c11, cerebellar and thalamic; c12, frontal eye fields and posterior parietal; c13, bilateral motor cortex; c14, cerebellar and thalamic; c15, occipital and posterior cingulate; c17, bilateral auditory and motor cortex; c18, bilateral cerebellar; c19, posterior DMN with the posterior cingulate; c20, bilateral cerebellar and occipital.

**Main figure 2:** Illustration of the interaction group (TSTH improvement <=50% or >50%) with time (baseline versus 1 year after SRS-T); Component 9, with insula and default-mode network IC with left claustrum and putamen- 2.1: boxplots with the median values for IC values corresponding left claustrum and putamen; 2.2: differences in IC between 1 year and baseline clearly separate the two groups, 1 and 2 and is statistically significant; 2.3: baseline IC values additionally correlate with baseline TSTH (Spearmann= 0.01); 2.4: differences in IC, 1 year after SRS-T, correlate with disease duration (Spearmann= 0.02);

**Main figure 3:** Artistic representation of the findings from interaction group with time, as presented in main figure 2; the respective roles of the relevant clusters are briefly synthesized: 3.1, claustrum; 3.2, putamen;

**Main figure 4:** Component 13, with bilateral sensorimotor cortex and frontal-eye fields, IC with right visual association area: 4.1: boxplots with the median values for corresponding IC values for right visual association area; 4.2: differences in IC between 1 year and baseline clearly separate the two groups, 1 and 2 and is statistically significant; 4.3: baseline IC values correlate with TSTH improvement (Spearmann= 0.01); 4.4: baseline IC values correlate with baseline head tremor score (Spearmann= 0.01); 4.5: differences in IC at 1 year after SRS-T correlate with lesion volume (Spearmann= 0.01); 4.6: baseline IC also correlate with lesion volume (Spearmann= 0.01)

**Main figure 5:** Artistic representation of the findings from interaction group with time, as presented in main figure 4; the respective roles of the relevant cluster are briefly synthesized: right visual association cortex

**Main figure 6:** Illustration of time-effect (baseline versus 1 year after SRS-T): Component 2, with right dorsal attention IC with left anterior VLPFC; 6.1: boxplots with the median values for corresponding IC values for left anterior VLPFC, as overall changes between baseline and 1 year after

SRS-T and further 6.2, separated by groups; 6.3: TSTH improvement relates to longitudinal changes in IC;

**Main figure 7:** Artistic representation of the findings from the main effect of time-point, as presented in main figure 6; the respective roles of the relevant clusters are briefly synthesized: left ventro-lateral prefrontal cortex;

**Main figure 8:** Component 9, with bilateral insula and default-mode network IC with the corresponding right visual association area (including V5); 9.1: boxplots with the median values for corresponding IC values for left anterior VLPFC, as overall changes between baseline and 1 year after SRS-T and further 9.2, separated by groups;

**Main figure 9:** Artistic representation of the findings from the main effect of time-point, as presented in main figure 8; the respective roles of the relevant cluster are briefly synthesized: fusiform gyrus

**Main figure 10:** Artistic representation of the main findings from main effect of group, as presented in supplementary figures 1, 2 and 3; the respective roles of the relevant anatomical areas are briefly synthesized.

**Supplementary figure 1:** Illustration of the effect of group on component 5, 6 and 11; for component 5, the corresponding clusters are left dentate (A), vermis (B) and right thalamus (pulvinar) (C) with axial (upper), coronal (middle) and sagittal reconstruction (lower); furthermore, illustration of the right pulvinar (C), with the respective boxplots and median values at baseline and 1 year, separated by groups, to show the effect; for component 6, the corresponding cluster is right parietal area (BA 7), with axial (left)), coronal (middle) and sagittal (right) reconstruction; the respective boxplots and median values at baseline and 1 year, separated by groups, to show the effect (below); for component 11, the corresponding clusters are right putamen (A), right thalamus (B) and left thalamus (C) with axial (upper), coronal (middle) and sagittal reconstruction (lower); further illustration of the right putamen and left thalamus FC values with the respective boxplots and median values at baseline and 1 year, separated by groups, to show the effect (below); for component 11, year, separated by groups, to show the respective boxplots and sagittal reconstruction (lower); further illustration of the right putamen and left thalamus FC values with the respective boxplots and median values at baseline and 1 year, separated by groups, to show the effect (below); with axial (upper), coronal (middle) and sagittal reconstruction (lower); further illustration of the right putamen and left thalamus FC values with the respective boxplots and median values at baseline and 1 year, separated by groups, to show the effect (below); with axial (upper), coronal (middle) and sagittal reconstruction (lower); further illustration of the right putamen and left thalamus FC values with the respective boxplots and median values at baseline and 1 year, separated by groups, to show the effect (below); with axial (upper), coronal (middle) and sagittal reconstruction (lower);

**Supplementary figure 2:** Illustration of the effect of group on component 13, 15 and 16; for component 13, the corresponding clusters are left frontal eye-fields (A), left dorso-lateral prefrontal (B), right (C) and left (D) supramarginal gyrus, with axial (upper), coronal (middle) and sagittal reconstruction (lower); furthermore, illustration of FC values for the left dorso-lateral, left frontal-eye fields and right supramarginal gyrus, with the respective boxplots and median values at baseline and 1

year, separated by groups, to show the effect (below); for component 15, the corresponding clusters are left retro-spenial cortex (A) and left angular gyrus (B), with axial (left), coronal (middle) and sagittal reconstruction (right); furthermore, illustration of FC values for both clusters, with the respective boxplots and median values at baseline and 1 year, separated by groups, to show the effect (below); for component 16, the corresponding clusters are right posterior cingulate (A), middle temporal area (B) and supramarginal gyrus (C), with axial (upper), coronal (middle) and sagittal reconstruction (lower); furthermore, illustration of FC values for posterior cingulate and left middle temporal area, with the respective boxplots and median values at baseline and 1 year, separated by groups, to show the effect (below);

**Supplementary figure 3:** Illustration of the effect of group on component 12, 18 and 19; for component 12, the corresponding clusters are left middle temporal area (A), left fusiform gyrus (B), left cerebellar (C), left angular gyrus (D), right supramarginal gyrus (E), right superior parietal lobule (F); for all of them, illustration of FC values, with the respective boxplots and median values at baseline and 1 year, separated by groups, to show the effect (below); for component 18, the corresponding clusters are left angular gyrus (A), left BA 7 parietal (B), left cerebellar (C), right anterior dorsal cingulate (D), right angular gyrus (E) and right ventral anterior cingulate (F); furthermore, illustration of FC values for left cerebellar and right anterior dorsal cingulate area, with the respective boxplots and median values at baseline and 1 year, separated by groups, to show the effect (below); for component 19, the corresponding clusters are left angular gyrus (A), left and right anterior dorsal cingulate area, with the respective boxplots and median values at baseline and 1 year, separated by groups, to show the effect (below); for component 19, the corresponding clusters are left angular gyrus (A), left parietal (B), left anterior dorsal cingulate (C), right posterior parietal (D), right angular gyrus (E) and right frontal eye fields (F); furthermore, illustration of FC values for left values for left anterior dorsal cingulate and frontal eye fields, with the respective boxplots and median values at baseline and 1 year, separated by groups, to show the effect (below)